Bacterial cellulose films with controlled microstructure–mechanical property relationships

A. Retegi · N. Gabilondo · C. Peña · R. Zuluaga ·
C. Castro · P. Gañan · K. de la Caba ·
I. Mondragon

Abstract Bacterial cellulose (BC) films with different porosities have been developed in order to obtain improved mechanical properties. After 13 days of incubation of *Gluconobacter xylinum* bacteria in static culture, BC pellicles have been set. BC films have been compression molded after water dispersion of BC pellicles and filtration by applying different pressures (10, 50, and 100 MPa) to obtain films with different porosities. Tensile behavior has been analyzed in order to discuss the microstructure–property relationships. Compression pressure has been found as an important parameter to control the final mechanical properties of BC films where slightly enhanced tensile strength and deformation at break are obtained increasing mold compression pressure, while modulus also increases following a nearly linear dependence upon film porosity. This behavior is related to the higher densification by increasing mold compression pressure that reduces the interfibrillar space, thus increasing the possibility of interfibrillar bonding zones. Network theories have been applied to relate film elastic properties with individual nanofiber properties.

Introduction

Cellulose is the most abundant biopolymer on earth, recognized as the major component of plant biomass but also a representative of microbial extracellular polymers. Bacterial cellulose (BC) belongs to specific products of primary metabolism. Cellulose is synthesized by bacteria belonging to the genera of *Acetobacter, Rhizobium*, *Agrobacterium*, and *Sarcina*. Its most efficient producers are Gram-negative, acetic acid bacteria *Acetobacter xylinum* (reclassified as *Gluconobacter xylinus*, Yamanaka et al. 2000), which have been applied as model microorganisms for basic and applied studies on cellulose. The formation of cellulose by laboratory bacterial cultures is an interesting and attractive biomimetic access to obtain pure cellulose for both organic and polymer chemists. By selecting the substrates, cultivation conditions, various additives, and finally the bacterial strain, it is possible to control the molar mass, molar mass distribution, and the supramolecular structure. Thus, it is possible to control important cellulose properties

A. Retegi · N. Gabilondo · C. Peña · K. de la Caba · I. Mondragon (✉)
Materials + Technologies Group, Polytechnic School, Dpto. Ingeniería Química y M. Ambiente, Universidad País Vasco/Euskal Herriko Unibertsitatea, Pza. Europa 1, 20018 Donostia-San Sebastián, Spain
e-mail: inaki.mondragon@ehu.es

R. Zuluaga · C. Castro · P. Gañan
New Materials Group, Universidad Pontificia Bolivariana
Circular 1 # 70-01, Medellin, Colombia

and also the course of biosynthesis (Klemm et al. 2005). Despite their identical chemical composition, the structure and mechanical properties of BC microfibrils differ from those of plant cellulose. BC microfibrils have high mechanical properties including tensile strength and modulus but also high water-holding capacity, moldability, crystallinity, and biocompatibility (Putra et al. 2008). Despite the excellent mechanical properties of BC films (Nakagaito et al. 2005) and BC composites (Gindl and Keckes 2004), values are far away from the possibilities offered by the high modulus of micro-fibrils, estimated to be around 140 GPa in the longitudinal direction (Nakagaito et al. 2005). For this reason, microstructural information is necessary for greater understanding of structure–mechanical property relationships and for applications both as a nanostructured material itself but also as a constituent combined with other materials.

Several groups have used different characterization techniques to investigate changes on bacterial cellulose properties (Watanabe et al. 1998) upon the cultivation conditions, but few works (Nishi et al. 1990) have analyzed the influence of film preparation conditions on their final behavior. In this work, a study on the influence of bacterial film preparation method on mechanical properties has been carried out analyzing the effect of compressive pressure in the porosity of BC films. Moreover, microstructure and morphology of BC have been investigated in order to establish microstructure–mechanical behavior relationships.

Materials and methods

BC films

Bacterial cellulose has been obtained in our laboratory from a *Gluconobacter xylinum* pellicle incubated for 13 days at 28 °C in a static culture containing 13.0% (wt/vol) sugar and agricultural pineapple residues in water adjusting pH with acetic acid to 3.3 in a glass flask. BC pellicles, grown in the air/liquid interface with a thickness of 0.5–0.7 cm, have been boiled in 5 wt% KOH solution for 60 min at 120 °C in order to remove non-cellulosic compounds and then thoroughly washed under running water for 2 days. Then, KOH-treated BC has been suspended in water (0.5 wt%), and mixture has been stirred for

48 h. Suspension has been vacuum filtered using nylon membrane filters (0.2-mm mesh) producing BC mats 25 mm in diameter that have been oven dried at 70 °C for 48 h between metal plates. Mats have been compressed at 10, 50, and 100 MPa at 70 °C in order to analyze the effect of compressive pressure in the mechanical properties of BC films.

Characterization methods

Atomic force microscopy (AFM)

Atomic force microscopy (Digital Instruments) having a NanoScope III controller with a multimode head has been used in order to characterize the size and morphological distribution of BC microfibrils in the films. For every sample, analysis has been performed in tapping mode (TM) in air under moderate conditions for recording height and phase images. Silicon canti-levers with a resonance frequency of about 200–400 kHz and a spring constant of 12–103 N/m have been used for imaging. A drop of BC/water suspension has been deposited onto freshly cleaved mica. Water has been removed before imaging by holding the sample in a silica gel ambient for 24 h. Surface images of compression molded BC films have been obtained sticking a piece of the film directly on AFM support.

X-ray diffractometry (XRD)

X-ray diffraction patterns have been measured using a X-ray diffractometer PW1710 (Philips) with CuKα radiation ($k = 1.54$ Å). Samples have been scanned from 10 to 40 2θ with a step size of 0.02 and 1.25 s time per step. The crystallinity index (CI) of BC films has been calculated from the reflected intensity data using Segal et al. method (1959):

$$CI = \frac{I_{020} - I_{am}}{I_{020}} \tag{1}$$

where I_{020} is the maximum intensity of the lattice diffraction, and I_{am} is the intensity at $2\theta = 18°$.

Polymerization degree (DP)

In order to estimate the average polymerization degree of bacterial cellulose, ASTM D 1795 method has been used. All experiments have been performed at 25 ± 0.5 °C using an Ubbelholde capillary

viscometer and cupriethylendiamine (CED) as a solvent. The intrinsic viscosity has been calculated from an abacus from the standard that relates concentration and relative viscosity (η_r), which has been calculated as follows:

$$\eta_r = \frac{\eta}{\eta_0} \approx \frac{t}{t_0} \qquad (2)$$

where t and t_0 are the efflux time for cellulose solution and solvent, respectively. The intrinsic viscosity is related to the DP by an empirical relationship for this polymer–solvent system, that is defined as $[\eta] = 2.42$ DP $^{0.76}$ (Marx-Figini 1987).

Porosity (P)

The porosity of BC films has been determined using the absolute density of cellulose ($\rho_c = 1.592$ g/mL) and film density (ρ_f) by the following equation (Mwaikambo and Ansell 2001):

$$P = \left(1 - \frac{\rho_f}{\rho_c}\right)100 \qquad (3)$$

Film density has been calculated in an Archimedes balance using benzene, with a density of 0.870 g/mL, as a solvent.

Tensile tests

Compressed films have been punched to prepare dogbone-shape specimens using Metrotec test cutter press. Tensile tests have been performed in a Minimat miniature mechanical testing machine using a 200 N load cell. The crosshead rate used in the test has been 1 mm/min, and the distance between grips used 22 mm. At least five specimens have been tested for each set of samples being the average values reported. As displacement has not been measured with an extensometer, it has been not possible to calculate real strain. Thereby, measured modulus values are lower than expected.

Results and discussion

Morphological and microstructural characterization of BC

Figure 1 reveals the surface of BC prepared in static culture before and after KOH treatment. Both samples show highly fibrous network-like structure consisting of ultrafine cellulose microfibrils. The typical lateral dimension is 30–40 nm in the case of BC pellicle and 20–30 nm for KOH-treated microfibrils. In both cases, the fibril length is several micrometers as the microfibril-ends are not apparent. The microstructure is similar in both cases; however, slight differences reveal that after KOH treatment, the width of microfibrils appears to be slightly smaller due to impurities elimination.

In order to study both microstructure and crystallinity of bacterial cellulose samples in the used culture medium, X-ray diffraction has been used. XRD patterns of as-obtained BC and after KOH treatment are shown in Fig. 2. XRD patterns of both BC, shown by the peaks observed at 14.5° and 22.7°, attributed to BC cultured in static culture (Borosysiak and Garbarczyk 2003; Jin et al. 2007; Yan et al. 2008), correspond to the typical profile of cellulose I allomorph. However, comparing with XRD profiles of plant cellulose (Zuluaga et al. 2009), the peak at 16.8° is unnoticeable. The difference might be an indication of different biosynthesis process. Whereas cellulose from plants is usually synthesized in rosette terminal complexes, *Gluconobacter* family bacteria synthesize cellulose in linear terminal complexes. According to this, rosette terminal complexes do not present any *preferred plane* between (110) and (110), and subsequently, the presence of both planes is equitative in plant cellulose. However, in the case of bacterial cellulose, as a consequence of the effect of preferred plane, cellulose molecules are parallelly oriented to the plane (110). This effect has been identified as "uniplanar orientation" tendency. Moreover, the drying process between glass plates can be one further reason for these differences due to induced microfibrils orientation. KOH treatment does not change the allomorphic structure as low alkali concentrations have been used. The peak at $2\theta = 22.7°$ is sharper for KOH-treated BC than for untreated, which is an indication of higher crystallinity degree in the structure of the treated sample (Alemdar and Sain 2008). The average crystallinity index (CI) value of KOH-treated BC is slightly higher than that of BC pellicle (68 to 71%, respectively) which may be related to higher cellulose purity after KOH treatment. Similar results were obtained for bacterial cellulose samples (63%) (Watanabe et al. 1998).
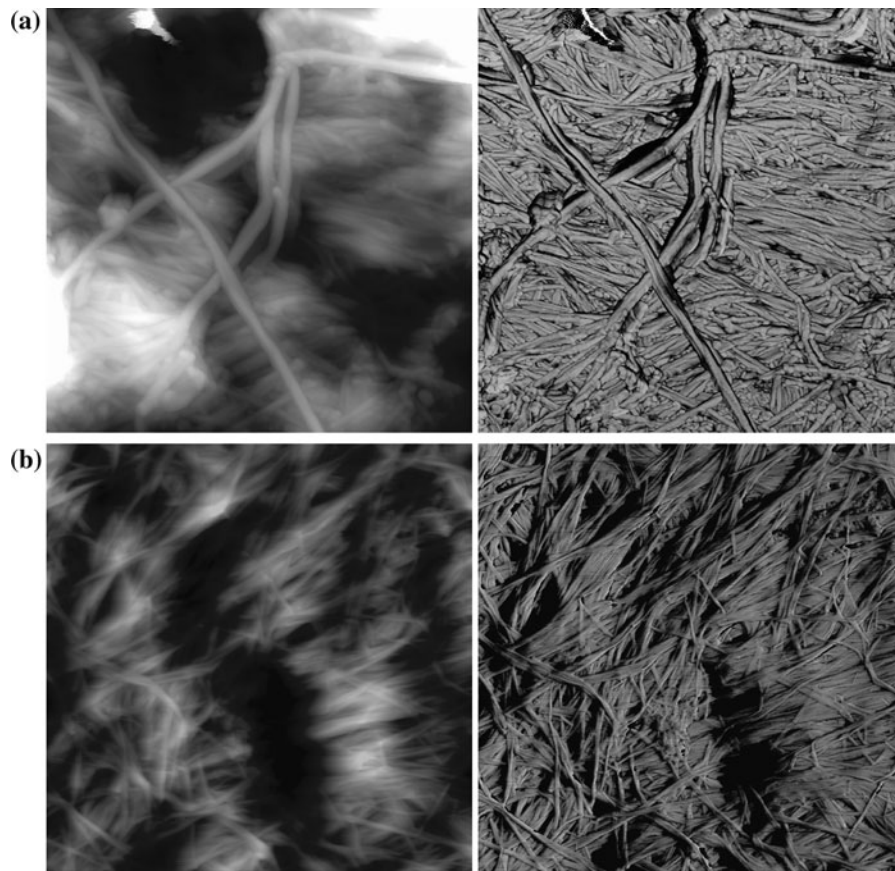
Fig. 1 3 μm × 3 μm AFM height/phase images of BC surfaces: **a** BC pellicle **b** KOH-treated BC film
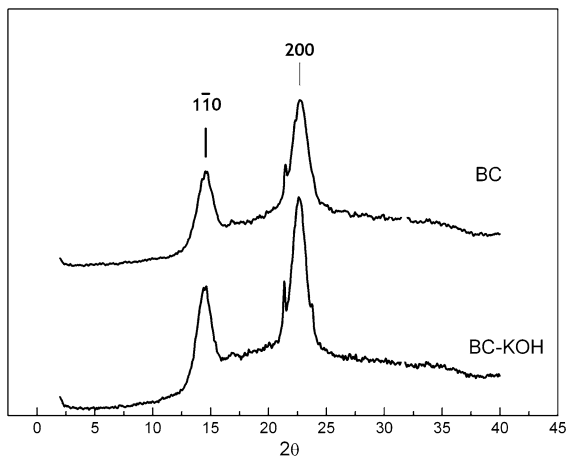

Fig. 2 XRD patterns of BC and KOH-treated BC pellicles

Characterization of BC films

Morphological and microstructural characterization

Figure 3 presents XRD profiles of BC films after compression molding under different compression pressures. No significant changes between the three profiles are observed, and also no great differences with XRD profile obtained for BC after incubation. This fact confirms that no microstructural changes are produced on the microfibrils during hot compression process. There is a slight interference of $16.5°$ peak that slightly increases as a consequence of hot-press process probably due to induced orientation. Moreover, as can be seen in Table 1, a significant increase in the CI from 71% for uncompressed BC film to
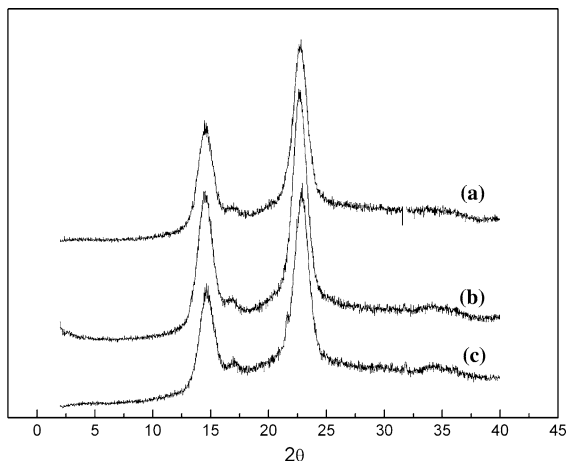
Fig. 3 XRD patterns of BC obtained upon different mold compression pressures: **a** 10 MPa **b** 50 MPa, and **c** 100 MPa

more than 84.3% for films is produced in the molding process. Similar increases in crystallinity were detected by other authors (Kumar and Kothari 1999) for low compression pressure-molded microcrystalline cellulose samples. This variation was attributed to the ability of cellulose crystallites to reorient themselves or to an increase in size of existing crystallite domains under compressional force. In addition, as shown in following paragraphs, as a consequence of the combination of the temperature–pressure effects, the decrease in the porosity in the film induces overall crystallinity.

In Fig. 4, surface images of BC films obtained under different compression pressures are presented. There is no preferential orientation of microfibrils in the film plane. In all cases, similar microfibrillar network-like structures are seen, but compared to the microstructure of Fig. 1, microfibrils seem to be more physically entangled with respect to each other. The same effect was visualized for cellulose nanopaper films obtained by water casting, as this method is known to be a very effective method to create strong secondary interfibrillar interaction including hydrogen

bonds (Henriksson et al. 2008). Moreover, AFM images reveal that morphology of the samples is slightly dependent on compression pressure, as can be seen in both BC microfibrils diameter change and reduced porosity. Increasing compression pressure, microfibril diameter is slightly increased, 5–10 nm difference, which might be due to local deformations on the BC film when compressed (Johansson and Alderborn 2001). Thus, related to those local deformations, it seems that porosity of the samples is slightly lower for higher compression pressure. Those results are in good agreement with porosity measurements where a decrease from 13.6 to 9.7% and 3.2% in porosity is observed for BC films obtained under 10, 50, and 100 MPa compression pressures, respectively (Table 1). Porosity values reported are slightly lower than those reported for other BC of plant cellulose films or sheets (Henriksson et al. 2008). An explanation for this fact may be the magnitude of the applied pressure, which in our work is remarkably higher.

Mechanical behavior

In Fig. 5, the stress–strain curves for BC films molded under different compression pressures are shown. Obtained data are presented in Table 1. Mechanical properties of cellulose films depend not only on fibril modulus but also on orientation and degree of interaction between microfibrils within the film obtained by water suspension casting (Henriksson et al. 2008). In this case, the methodology used for film preparation has been the same up to the final stage where different compression pressures have been applied. The curves follow an initial linear zone up to deviation from elasticity takes place, which occurs around 0.5–0.7% apparent strain values in all cases, followed by a second linear region up to fracture. Hsieh et al. (2008) prepared BC films for tensile testing and related the non-linear curve to the breakdown within the network of fibers during deformation (e.g., bond breaking, fiber pull out). BC films molded with

Table 1 BC film properties under different compression molding pressures

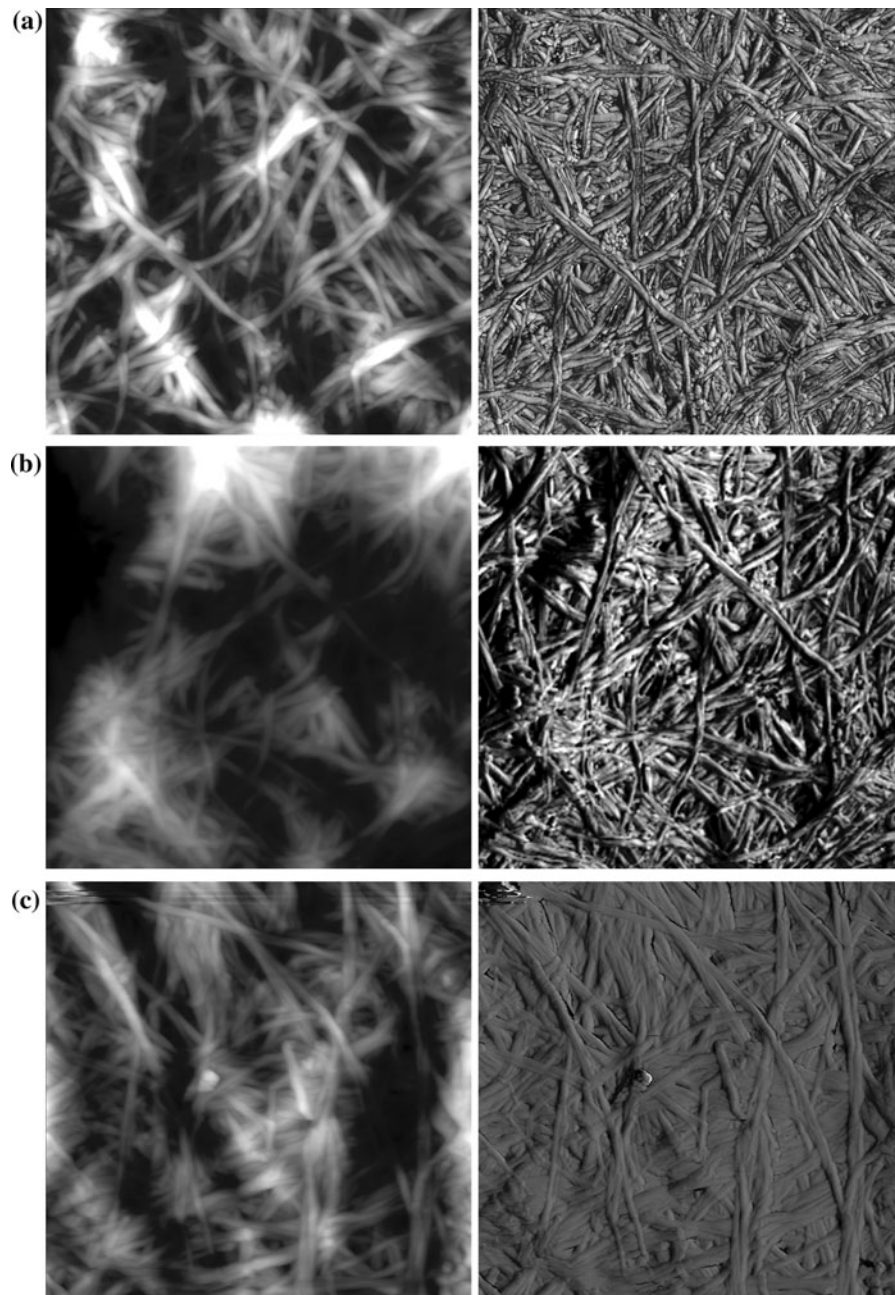| Sample	Porosity (%)	CI^{XRD} (%)	Tensile modulus (GPa)	Tensile strength (MPa)	Elongation at break (%)
BC 10 MPa	13.6	86.5	9.8 ± 0.8	87.5 ± 11.0	1.1 ± 0.1
BC 50 MPa	9.7	87.2	10.5 ± 1.0	165.0 ± 8.0	2.5 ± 0.1
BC 100 MPa	3.2	84.3	10.6 ± 0.5	182.5 ± 12.5	3.8 ± 0.2

Fig. 4 3 μm × 3 μm AFM height/phase images of BC films under different compression pressures: **a** 10 MPa, **b** 50 MPa, and **c** 100 MPa

different compression pressures follow similar features but without second linear region in the 10 MPa compressed film. In the case of 50- and 100-MPa compressed films, increasing compression pressure films show higher deformation at break and consequently higher tensile strength. As can be seen in

Table 1, BC films show high modulus value attributed to the uniform, continuous, and straight nanoscale network of cellulosic elements in-plane oriented via the compression of BC pellicles (Nakagaito et al. 2005). Moreover, increasing compression pressure, higher tensile modulus is obtained. Henriksson et al.
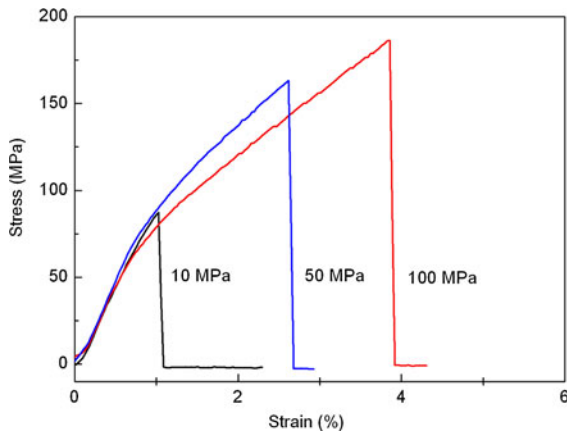
Fig. 5 Stress–strain curves for BC films obtained under different mold compression pressures
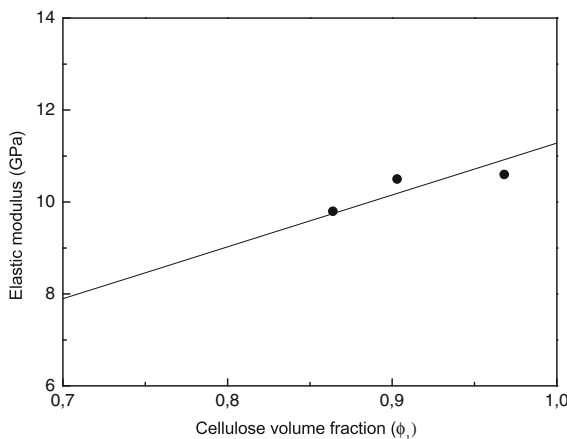

Fig. 6 Elastic modulus of BC films vs. cellulose volume fraction on the films: (*bullet*) experimental data and (*dash*) mixture model

(2008) obtained cellulose nanopaper films with different porosities after water suspension casting using different DP and found that elastic modulus did not follow any tendency as similar modulus values were obtained. This conclusion is also supported by other studies where elastic modulus of BC is attributed to the planar and straight orientation of the continuous and dimensionally uniform three-dimensional cellulose structure (Eichhorn and Young 2001; Nakagaito and Yano 2004). Even microfibril diameter is not considered an important factor on the elastic modulus contribution, Gushados et al. (2005) measured the elastic modulus of single bacterial cellulose fibers. Using AFM with diameter ranging from 27 to 88 nm, obtaining a constant value of 78 GPa. Other

parameters as crystallinity may play a more important contribution in the modulus of semicrystalline or composite materials such as cellulose where the elastic modulus is a combination of crystalline (128 GPa) and amorphous (5 GPa) contribution (Iwamoto et al. 2007; Gushados et al. 2005). The first one contributes to the elasticity of the material and the second one to the flexibility and plasticity of bulk materials. Based on Reuss model, Eichhorn and Young (2001) developed a relationship between elastic modulus and percent crystallinity and predicted a modulus of 12 GPa for a 60%-crystallinity cellulose mat.

On the contrary, as mentioned above, Young modulus of BC films is dependent upon the applied compression pressure. As a first approach, a mixture law has been applied to estimate the elastic modulus evolution with the porosity of the films. Film modulus can be calculated as:

$$E_{\text{film}} = \Phi_1 E_1 + \Phi_2 E_2 \qquad (4)$$

where Φ_1 is the cellulose volume fraction, E_1 BC elastic modulus, and Φ_2 air volume fraction, and E_2 air elastic modulus. Taking into account that air does not contribute to the modulus, mixtures law fits rather well with experimental values, as can be observed in Fig. 6, in which modulus is plotted as a function of cellulose content in the films.

However, for bacterial cellulose films, network theories can be applied, in order to attempt to describe the elastic properties of films in terms of individual microfiber properties and the arrangement of nanofiber and microfiber bonds. The microfiber is assumed to be embedded in the network through a bonding zone. The joint or bonding area comes from both the synthesizing process during cultivation of bacterial cellulose, and it can increase through film production and compression molding process. Through compression, the surface of the microfiber is covered, and microfiber network is coupled. If assumed that all fibers lie in the plane of the film, they can be modeled as plane stress structures. Moreover, by also supposing random distributions of microfibers and mean values for fiber properties, several 2D network models can be applied in order to relate film properties with individual microfiber properties. Cox (1952) developed the original theory for a random fiber network consisting of long straight fibers attached at the ends, assuming that the strain in the fibers was equal to the strain in the sheet, a uniform strain theory. Cox proposed:

$$E_{\text{film}} = \frac{1}{3}\frac{\rho_{\text{film}}}{\rho_{\text{fibril}}}E_{\text{fibril}} \qquad (5)$$

where E_{film} is the longitudinal modulus of the film, ρ_{film} is the density of the film, ρ_{fibril} is the density of each cellulose microfiber (1.592 g/mL), and E_{fibril} is the longitudinal modulus of cellulose microfiber. More recently, using Krenchel analysis (1964), the modulus of single bacterial cellulose filament or fibril can be obtained. Krenchel method is based on the fact that for a 2D in-plane random distribution of fibers, an efficiency factor (η_0) for the stress factor does exist, which is generally taken as 3/8 and can be related as follows:

$$E_{\text{film}} = \eta_0 E_{\text{fibril}} \qquad (6)$$

The calculated values for the elastic modulus of bacterial cellulose microfiber are in the range of 28.2–31 GPa (Krenchel-Cox network theories), that slightly lower that one would be expected from its crystallinity index value (71%, calculated by X-ray). Indeed, according to McCullough model (1976), adapted by Ganster et al. (1994), where the contribution of the crystalline, E_c (128 GPa), and amorphous moduli, E_a (5 GPa), and a contiguity parameter, ξ, which describes the coupling of the crystalline and amorphous components are included, the following equation can be applied:

$$E_{\text{fibril}} = \frac{E_a(1 + \xi V_c \Xi)}{1 - V_c \Xi} \qquad (7)$$

where V_c is the crystallinity, and Ξ is defined as:

$$\Xi = \frac{E_c - E_a}{E_c - \xi E_a}. \qquad (8)$$

The contiguity parameter best fits with a five value, indicating that cellulose crystallites are much longer than wide. According to Ganster model, the apparent modulus of our bacterial cellulose, with a crystallinity index of 71%, should be near 37 GPa.

Henriksson et al. (2008) proposed that for high DP cellulose (higher than 2,500 DP), failure occurs by covalent bond breakage instead of slippage of the extended cellulose chains. Taking into account BC produced in this work shows a DP value of 2,850 that is in the range of typical BC, the effect of covalent bond should be prevalent. Moreover, remarked that films were prepared from water suspensions, strong secondary interfibrillar interaction including hydrogen bonds can be expected. These findings support the mechanistic view used by Johansson et al. (1998) in order to correlate strength and compression pressure with an increase in the bonding zone area. Increasing compression pressure, porosity is reduced, and so the area of bonding zones increases, and consequently the probability to covalent bonding between adjacent and entangled microfibrils also increases. Therefore, stress applied to the films is more likely to be transferred during testing (Eichhorn et al. 2001). Also, Yamanaka et al. (2000) stated that improved mechanical properties and more extensive hydrogen bonding were produced when a cellulosic mass was heat-pressed. Our findings support the importance of interfibrillar bonding for strength and elongation at break, since enhanced mechanical behavior can be set when low-porosity films are obtained.

Conclusions

Bacterial cellulose films with dissimilar porosities (different compression pressures) were prepared in order to analyze microstructure–mechanical behavior relationships. The combination of several analysis techniques allowed explaining the behavior of BC films in order to apply them in high performance applications. BC pellicles, obtained in static culture, presented high DP, 2,850, being cellulose I allomorph. BC films obtained after water casting showed a uniformly random in-plane distribution of network-like structure where high aspect ratio microfibrils were physically entangled. Moreover, all compressed BC films presented the same cellulose I allomorph but with higher crystallinity index than BC pellicle. As a consequence, films presented excellent mechanical behavior. Higher mechanical properties were obtained for higher compression pressures with increased tensile strength and elongation at break. The reason for improved mechanical properties can be attributed to the reduced porosity upon increasing compression that increases the probability of interfibrillar bonding. The lower film porosity at higher compression pressure has a clear effect on elastic modulus values. Several network theories have been applied to relate film elastic properties with individual nanofiber properties, and the accordance between them has been rather good. Indeed, the proposed film fabrication methodology opens a new way to the

design of nanostructured materials with high mechanical performance using a biodegradable material from a renewable resource as bacterial cellulose.

References

Alemdar A, Sain M (2008) Biocomposites from wheat straw nanofibres: morphology, thermal and mechanical properties. Comp Sci Technol 68:557–565

Borosysiak S, Garbarczyk J (2003) Applying the WAXS method to estimate the supermolecular structure of cellulose fibres after mercerisation. Fibres & Text 11:104–106

Cox HL (1952) The elasticity and strength of paper and other fibrous materials. Brit J Appl Phys 3:72–79

Eichhorn SJ, Young RJ (2001) The Young's modulus of a microcrystalline cellulose. Cellulose 8:197–207

Eichhorn SJ, Sirichaisit J, Young RJ (2001) Deformation mechanisms in cellulose fibres, paper and wood. J Mater Sci 36:3129–3135

Ganster J, Fink H-P, Fraatz J, Nywlt M (1994) Relation between structure and elastic constants of man-made cellulosic fibres: I. A two phase anisotropioc model with contiguity parameter. Acta Polymer 45:312–318

Gindl W, Keckes J (2004) Tensile properties of cellulose acetate butyrate composites reinforced with bacterial cellulose. Comp Sci Technol 64:2407–2413

Gushados G, Wan W, Hutter JL (2005) Measurement of the elastic modulus of single bacterial cellulose fibers using atomic force microscopy. Langmuir 21:6642–6646

Henriksson M, Berglund LA, Isaksson P, Lindström T, Nishino T (2008) Cellulose nanopaper structures of high toughness. Biomacromolecules 9:1579–1585

Hsieh YC, Yano H, Nogi M, Eichhorn S (2008) An estimation of the Young's modulus of bacterial cellulose filaments. Cellulose 15:507–513

Iwamoto, Nakagaito AN, Yano H (2007) Nano-fibrillation of pulp fibers for the processing of transparent nanocomposites. Appli Phys A 89:461–466

Jin H, Zha C, Gu L (2007) Direct dissolution of cellulose in NaOH/thiourea/urea aqueous solution. Carbohydr Res 342:851–858

Johansson B, Alderborn G (2001) The effect of shape and porosity on the compression behaviour and tablet forming ability of granular materials formed from microcrystalline cellulose. Eur J Pharm Biopharm 52:347–357

Johansson B, Nicklasson F, Alderborn G (1998) Effect of pellet size on degree of deformation and densification during compresion and on compatibility of microcrystalline cellulose pellets. Int J Pharm 52:347–357

Klemm D, Heublein B, Fink HP, Bohn A (2005) Cellulose: fascinating biopolymer and sustainable raw material. Angew Chem Int Ed 44:3358–3393

Krenchel H (1964) Fibre reinforcement. Akademisk Forlag, Copenhagen

Kumar V, Kothari SH (1999) Effect of compressional force on the crystallinity of directly compressible cellulose excipients. Int J Pharm 177:173–182

Marx-Figini M (1987) Evaluation of the accessibility of celluloses by intrinsic viscosity ratio. Polym Bull 17:225–229

McCullough RL, Wu CT, Seferis JC, Lindenmeyer PH (1976) Predictions of limiting mechanical performance for anisotropic crystalline polymers. Polym Eng Sci 16:371–387

Mwaikambo LY, Ansell MP (2001) The determination of porosity and cellulose content of plant fibres by density method. J Mater Sci Lett 20:2095–2096

Nakagaito AN, Yano H (2004) The effect of morphological changes from pulp fiber towards nano-scale fibrillated cellulose on the mechanical properties of high-strength plant fiber based composites. Appl Phys A: Mater Sci Process 78:547–552

Nakagaito AN, Iwamoto S, Yano H (2005) Bacterial cellulose: the ultimate nano-scalar cellulose morphology for the production of high-strength composites. Appl Phys A: Mater Sci Process 80:93–97

Nishi Y, Uryu M, Yamanaka S, Watanabe K, Kitamura N, Iguchi M, Mitsuhashi S (1990) The structure and mechanical properties of sheets prepared from bacterial cellulose. J Mater Sci 25:2997–3001

Putra A, Kakugo A, Furukawa H, Gong JP, Osada Y (2008) Tubular bacterial cellulose gel with oriented fibrils on the curved surface. Polymer 49:1885–1891

Segal L, Creely J, Martin A, Conrad C (1959) An empirical method for estimating the degree of crystallinity of native cellulose using the X-ray diffractometer. Text Res J 29:786–794

Watanabe K, Tabuchi M, Morinaga Y, Yoshinaga F (1998) Structural features and properties of bacterial cellulose produced in agitated culture. Cellulose 5:187–200

Yamanaka S, Ishihara M, Sugiyama J (2000) Structural modification of bacterial cellulose. Cellulose 7:213–225

Yan Z, Chen S, Wang H, Wang B, Wang C, Jiang J (2008) Cellulose synthesized by *Acetobacter xylinum* in the presence of multi-walled carbon nanotubes. Carbohydr Res 343:73–80

Zuluaga R, Putaux JL, Cruz J, Vélez J, Mondragon I, Gañan P (2009) Cellulose microfibrils from banana rachis: effect of alkaline treatments on structural and morphological features. Carbohydr Polym 76:51–59